Classical stochastic systems with fast-switching environments: Reduced master equations, their interpretation, and limits of validity

Peter G. Hufton,[1] Yen Ting Lin,[1,2] and Tobias Galla[1]

[1]*Theoretical Physics, School of Physics and Astronomy, University of Manchester, Manchester M13 9PL, United Kingdom*

[2]*Center for Nonlinear Studies and Theoretical and Biophysics Group, Theoretical Division, Los Alamos National Laboratory,
Los Alamos, New Mexico 87545, USA*

We study classical Markovian stochastic systems with discrete states, coupled to randomly switching external environments. For fast environmental processes we derive reduced dynamics for the system itself, focusing on corrections to the adiabatic limit of infinite timescale separation. We show that this can lead to master equations with bursting events. Negative transition rates can result in the reduced master equation, leading to unphysical short-time behavior. However, the reduced master equation can describe stationary states better than a leading-order adiabatic calculation, similar to what is known for Kramers-Moyal expansions in the context of the Pawula theorem [R. F. Pawula, Phys. Rev. **162**, 186 (1967); H. Risken and H. Vollmer, Z. Phys. B **35**, 313 (1979)]. We provide an interpretation of the reduced dynamics in discrete time and a criterion for the occurrence of negative rates for systems with two environmental states.

I. INTRODUCTION

Physical and biological systems can never be fully isolated from their environment. This includes the dynamics of microbes in time-varying external conditions (e.g., antibiotic treatment) [1–4] or protein production in gene regulatory networks, influenced by the stochastic binding and unbinding of promoters [5–9]. Other examples can be found in models of evolutionary dynamics [10–13], the spread of diseases [14], ecology and population dynamics [15–18]. Many of the models of these phenomena contain two types of randomness: one intrinsic to the system itself and another generated by the noise in the environmental dynamics. The study of open quantum systems defines an entire area of research [19–21].

These examples share a common structure: There is the system proper and the environment, and a coupling between them; this interaction can act either in one way or in both directions. In such situations it is often not possible (or desirable) to track and analyze in detail the dynamics of the system *and* that of the environment. Instead the focus is on deriving reduced dynamics for the system itself, which in some way accounts for the influence of the environment on the system. Work on open quantum systems, for example, focuses on understanding the dynamics of reduced density matrices after integrating out the environment [19–21].

Existing work on open classical systems includes those described by stochastic differential equations coupled to continuous environments [10,22–24] and deterministic models with discrete external noise [25–27]. A specific case of Brownian particles subject to random external gating is considered in Ref. [28]. In chemical or biological systems the quasi-steady-state approximation or related adiabatic reduction techniques can be used to eliminate fast reactions [29,30].

In this paper we consider open stochastic systems with discrete states. While some of our work is applicable more generally, we mostly focus on populations of interacting individuals. We will often use the words "system" and "population" synonymously. Examples we have in mind are chemical reaction systems with discrete molecules, or populations in biological systems, composed of members of different species. For a fixed environment, such a system is described by a (classical) master equation defined by the transition rates between its discrete states. These transitions are typically events in which particles are produced or removed from the population, or in which a particle of one type is converted into another type. In biological populations they can represent birth or death events. We are interested in cases in which such a population is coupled to an external environment, which also takes discrete states. The environmental states in turn affect the transition rates within the population.

Our aim is to study the reduced dynamics of such systems after the environmental dynamics are integrated out. In particular, we focus on the limit in which the environmental dynamics are fast compared to those of the population, but where the separation of timescales is not infinite. We ask what the reduced dynamics looks like, if and how it can be interpreted, and how one might go about simulating it efficiently. In the following paper [31] we build on these results and carry out expansions of the reduced dynamics for weak intrinsic and environmental noise.

The remainder of the paper is organized as follows. In Sec. II we introduce the type of model we address, a classical stochastic system with discrete states coupled to an external environment, also with discrete states. We derive an effective master equation in the limit of fast timescales of the environmental switching; specifically, our analysis includes next-order corrections to the adiabatic limit of infinitely fast environments. In Sec. III we focus on the case of two environmental states and use a simple example of a population with two species and two environmental states to illustrate the reduced dynamics. We show how negative transition "rates"

can arise in the reduced master equation. Section IV then focuses on the analysis of this reduced master equation in continuous time. We show that negative solutions can result at short timescales for a certain initial condition. We comment on the origin of these unphysical transients and demonstrate that the reduced master equation can nevertheless describe stationary distributions at long times with more accuracy than the dynamics in the adiabatic limit. In Sec. V we provide a physical interpretation of the reduced dynamics in discrete time. Specifically we show that a discrete-time process with reaction rates drawn from a Gaussian distribution at each time step can capture dynamical features of the full dynamics of the system and environment. In Sec. VI we establish a criterion for the occurrence of negative rates for models in which the environmental dynamics has two states and is independent of the state of the population. We summarize our results in Sec. VII and discuss their relevance and future lines of research which follow on from the work presented here.

II. GENERAL DEFINITIONS AND REDUCED MASTER EQUATION

A. Model

We focus on a classical system with discrete states, labeled ℓ, which is coupled to an environment also taking discrete states, which we label σ. The system and the environment evolve in continuous time. The dynamics of the system itself depends on the current state of the environment. The environment in turn switches between its states, with transition rates which can depend on the state ℓ of the system. The combined dynamics of system and environment is then governed by the master equation

$$\frac{d}{dt}p(\ell,\sigma,t) = \mathcal{M}_\sigma p(\ell,\sigma,t) + \lambda \sum_{\sigma'} A_{\sigma'\to\sigma}(\ell)p(\ell,\sigma',t),$$

(1)

where $p(\ell,\sigma,t)$ is the joint probability of finding the system in state ℓ and the environment in state σ at time t. The object $\mathcal{M}_\sigma$ is an operator and determines how the state of the system can change when the environment is in state σ. More specifically, the effect of the operator can be written in the form

$$\mathcal{M}_\sigma p(\ell,\sigma,t) \equiv \sum_{\ell'} R^{(\sigma)}_{\ell'\to\ell}p(\ell',\sigma,t).$$

(2)

The matrix element $R^{(\sigma)}_{\ell'\to\ell}$ describes the rate at which the system transitions from state ℓ' to state ℓ when the environment is in state σ. For a chemical reaction system, the types of allowed transitions are specified by the stoichiometric coefficients; together with associated reaction rates, these determine the transition matrix. In the context of population dynamics the matrix $R^{(\sigma)}_{\ell'\to\ell}$ is defined by the underlying birth and death processes (see, e.g., Refs. [32,33]).

The second term in Eq. (1), proportional to λ, characterizes the environmental switching. The rate with which the environment transitions from state σ to state σ' is $\lambda A_{\sigma\to\sigma'}(\ell)$. In the most general setup, these can depend on the state ℓ of the system. We write $\lambda \mathbf{A}(\ell)$ for the corresponding transition matrix. The prefactor $\lambda > 0$ has been introduced

to parametrize the timescale of the environment, relative to the internal dynamics of the population. To fix the diagonal elements of both transition matrices, we use the convention $R^{(\sigma)}_{\ell\to\ell} = -\sum_{\ell'\neq\ell} R^{(\sigma)}_{\ell\to\ell'}$ and $A_{\sigma\to\sigma}(\ell) = -\sum_{\sigma'\neq\sigma} A_{\sigma\to\sigma'}(\ell)$.

We introduce the notation $\Pi(\ell,t) = \sum_\sigma p(\ell,\sigma,t)$ for the marginal of the probability distribution after integrating out the environment. The general objective of this paper is to study the time evolution of this marginal distribution in the limit of fast-switching environments $\lambda \gg 1$.

B. Simplification in the adiabatic limit

We first consider the so-called adiabatic limit of infinitely fast environmental switching $\lambda \to \infty$. In this limit and similar to [25], we find, from Eq. (1),

$$\sum_{\sigma'} A_{\sigma'\to\sigma}(\ell)p(\ell,\sigma',t) = 0$$

(3)

for all ℓ. Writing the joint distribution $p(\ell,\sigma,t)$ in terms of the marginal $\Pi(\ell,t)$ and a conditional probability $\rho(\sigma|\ell,t)$, we have $p(\ell,\sigma,t) = \rho(\sigma|\ell,t)\Pi(\ell,t)$. Substituting this into Eq. (3) we find

$$\sum_{\sigma'} A_{\sigma'\to\sigma}(\ell)\rho^*(\sigma'|\ell) = 0,$$

(4)

for all ℓ, for the stationary distribution of the environment conditioned on the state of the system. We label this stationary distribution by an asterisk. In the adiabatic limit we then have

$$p(\ell,\sigma,t) = \rho^*(\sigma|\ell)\Pi(\ell,t).$$

(5)

We will use this relation as a starting point for further analysis; in the course of this analysis we also obtain the reduced dynamics for $\Pi(\ell,t)$ in the adiabatic limit.

C. Reduced master equation for large but finite separation of timescales

Our next aim is to derive reduced dynamics in the limit of fast environmental switching, but keeping the timescale separation finite (i.e., λ large, but finite). Specifically, the objective is to derive a closed equation for the time evolution of the distribution of states $\Pi(\ell,t)$. This is done by performing an expansion of the joint master equation for the system and environment in powers of the timescale separation λ^{-1}. We then retain the leading and subleading terms and integrate out the environment. The algebraic steps are similar to those in Ref. [25], in which the authors work in the context of piecewise-deterministic Markov processes. We carry out the calculation starting from a system with discrete states ℓ. As we will see below, this leads to interesting features of the reduced dynamics, not necessarily seen for continuous states.

To separate leading-order terms from subleading contributions we start with the decomposition

$$p(\ell,\sigma,t) = \rho^*(\sigma|\ell)\Pi(\ell,t) + \frac{1}{\lambda}w_\sigma(\ell,t).$$

(6)

The term $w_\sigma(\ell,t)$ describes deviations from the adiabatic limit [Eq. (5)], due to a finite timescale of the environment. It includes corrections of order λ^{-1} and higher, i.e., $w_\sigma(\ell,t)$ is in itself a power series. Because of normalization, this ansatz

requires $\sum_\sigma w_\sigma(\ell, t) = 0$ for all ℓ. We proceed by inserting Eq. (6) into Eq. (1) and obtain

$$\rho^*(\sigma|\ell)\frac{d}{dt}\Pi(\ell, t) + \frac{1}{\lambda}\frac{d}{dt}w_\sigma(\ell, t)$$
$$= \mathcal{M}_\sigma[\rho^*(\sigma|\ell)\Pi(\ell, t)] + \sum_{\sigma'}A_{\sigma'\to\sigma}(\ell)w_{\sigma'}(\ell, t)$$
$$+ \frac{1}{\lambda}\mathcal{M}_\sigma w_\sigma(\ell, t), \tag{7}$$

where one further term has been eliminated using Eq. (4). Next we sum over the environmental states σ for each ℓ. We find

$$\frac{d}{dt}\Pi(\ell, t) = \sum_\sigma \mathcal{M}_\sigma[\rho^*(\sigma|\ell)\Pi(\ell, t)] + \frac{1}{\lambda}\sum_\sigma \mathcal{M}_\sigma w_\sigma(\ell, t). \tag{8}$$

Once the $w_\sigma(\ell, t)$ are expressed in terms of $\Pi(\ell, t)$, this equation describes the time evolution of $\Pi(\ell, t)$, valid to subleading order in λ^{-1}.

To find the leading contribution to $w_\sigma(\ell, t)$ we collect the terms of order $(1/\lambda)^0$ in Eq. (7),

$$\sum_{\sigma'}A_{\sigma'\to\sigma}(\ell)w_{\sigma'}(\ell, t) = \rho^*(\sigma|\ell)\sum_{\sigma'}\mathcal{M}_{\sigma'}[\rho^*(\sigma'|\ell)\Pi(\ell, t)]$$
$$- \mathcal{M}_\sigma[\rho^*(\sigma|\ell)\Pi(\ell, t)], \tag{9}$$

where we have used Eq. (8) to further simplify the result. Effectively, we have disregarded terms of order λ^{-1} in Eq. (7). This procedure indicates that the $w_\sigma(\ell, t)$ are to be obtained as the solution of Eq. (9), subject to $\sum_\sigma w_\sigma(\ell, t) = 0$ for all ℓ and t. The truncation of higher-order terms leads to an error in Eq. (9) of order λ^{-1}. We note that in specific cases master equations for the system can be obtained in closed form without truncation (examples can be found in Refs. [34,35]). These usually rely on specific properties of the model, such as linearity. Equations (8) and (9), while constituting an approximation to subleading order in λ^{-1}, hold more generally; we have not made significant restrictions on the dynamics of the system (i.e., on the operators $\mathcal{M}_\sigma$). For example, the approach can be used for population dynamics defined by birth and death processes, and with an arbitrary number of species. It can also be applied to spatially extended or networked systems.

III. TWO ENVIRONMENTAL STATES: REDUCED MASTER EQUATION AND BASIC EXAMPLE

A. Environmental dynamics independent of the state of the system

We now make a simplifying assumption and consider the case in which the environmental switching dynamics is independent of the state of the population. That is to say, the transition rate matrix $A_{\sigma\to\sigma'}$ does not depend on ℓ. In this case, the stationary distribution of the environment in the adiabatic limit is independent of the state of population, i.e., $\rho^*(\sigma|\ell) = \rho^*_\sigma$. The more general case is discussed further in Appendix A and also in a further example in [31].

In this simplified case the dynamics in the adiabatic limit is given by

$$\frac{d}{dt}\Pi(\ell, t) = \mathcal{M}_{\text{avg}}\Pi(\ell, t), \tag{10}$$

where $\mathcal{M}_{\text{avg}} = \sum_{\sigma'}\rho^*_{\sigma'}\mathcal{M}_{\sigma'}$ is an effective average operator. Equation (10) is obtained from Eq. (8) by sending $\lambda \to \infty$ and using $\rho^*(\sigma|\ell) = \rho^*_\sigma$. Equation (9), on the other hand, reduces to

$$\sum_{\sigma'}A_{\sigma'\to\sigma}w_{\sigma'}(\ell, t) = \rho^*_\sigma[\mathcal{M}_{\text{avg}} - \mathcal{M}_\sigma]\Pi(\ell, t). \tag{11}$$

While the above procedure applies to an arbitrary number of discrete environmental states, it is useful to look at the case of two states, which we label $\sigma = 0$ and $\sigma = 1$. We then have $w_0(\ell, t) = -w_1(\ell, t)$ for all ℓ and t. To shorten the notation, we write k_0 and k_1 for the switching rates $A_{1\to0}$ and $A_{0\to1}$, respectively. In the adiabatic limit, the probabilities of finding the environment in each of its two states are then given by

$$\rho^*_0 = \frac{k_0}{k_0 + k_1}, \quad \rho^*_1 = \frac{k_1}{k_0 + k_1}. \tag{12}$$

From Eq. (11) we obtain

$$w_\sigma(\ell, t) = \frac{k_\sigma}{(k_0 + k_1)^2}[\mathcal{M}_\sigma - \mathcal{M}_{\text{avg}}]\Pi(\ell, t). \tag{13}$$

Substituting in Eq. (8) and simplifying, we arrive at

$$\frac{d}{dt}\Pi(\ell, t) = \mathcal{M}_{\text{avg}}\Pi(\ell, t) + \frac{1}{2}\frac{\theta^2}{\lambda}(\mathcal{M}_0 - \mathcal{M}_1)^2\Pi(\ell, t), \tag{14}$$

where

$$\theta^2 = \frac{2k_0 k_1}{(k_0 + k_1)^3}. \tag{15}$$

For systems with two environmental states and with population-independent environmental switching, Eq. (14) is a general result approximating the dynamics in the limit of fast switching. It captures the time evolution of $\Pi(\ell, t)$ up to and including subleading terms in λ^{-1}. We discuss limitations to its physical interpretation below. Despite these limitations, we will refer to Eq. (14) (and its analog for more complicated setups) as a reduced master equation. An expression similar to Eq. (14) was derived in Ref. [25] for systems with continuous states. We note that $(\mathcal{M}_0 - \mathcal{M}_1)^2 = (\mathcal{M}_0^2 - 1) + (\mathcal{M}_1^2 - 1) - (\mathcal{M}_0\mathcal{M}_1 - 1) - (\mathcal{M}_1\mathcal{M}_0 - 1)$, indicating that Eq. (14) preserves total probability, i.e., $\frac{d}{dt}\sum_\ell \Pi(\ell, t) = 0$.

B. Example: Population with two species

1. Reduced dynamics

We next consider a specific example. This will help reveal a number of interesting features which can emerge in the reduced dynamics.

The example describes a population with two types of particles, labeled A and B. Particles of either type are removed with constant per capita rates γ and δ, respectively, and are created with rates $\Omega\alpha_\sigma$ and $\Omega\beta_\sigma$. These production rates depend on the state of the environment, as indicated by the subscript. The population takes states $\ell = (n_A, n_B)$, where n_A

is the number of particles of type A and n_B the number of particles of type B. We then have operators

$$\mathcal{M}_\sigma = \Omega\alpha_\sigma(\mathcal{E}_A^{-1} - 1) + \gamma(\mathcal{E}_A - 1)n_A$$
$$+ \Omega\beta_\sigma(\mathcal{E}_B^{-1} - 1) + \delta(\mathcal{E}_B - 1)n_B, \qquad (16)$$

where $\mathcal{E}_A f(n_A, n_B) = f(n_A + 1, n_B)$ and similarly for $\mathcal{E}_B$. The switching between environmental states is the same as in the preceding section. Using Eq. (14) we find, to subleading order in λ^{-1},

$$\frac{d}{dt}\Pi = \gamma(\mathcal{E}_A - 1)n_A\Pi + \delta(\mathcal{E}_B - 1)n_B\Pi$$
$$+ \Omega\alpha_{\text{eff}}(\mathcal{E}_A^{-1} - 1)\Pi + \Omega\beta_{\text{eff}}(\mathcal{E}_B^{-1} - 1)\Pi$$
$$+ \frac{\Omega^2\theta^2}{2\lambda}(\Delta\alpha)^2(\mathcal{E}_A^{-2} - 1)\Pi$$
$$+ \frac{\Omega^2\theta^2}{2\lambda}(\Delta\beta)^2(\mathcal{E}_B^{-2} - 1)\Pi$$
$$+ \frac{\Omega^2\theta^2}{\lambda}\Delta\alpha\Delta\beta(\mathcal{E}_A^{-1}\mathcal{E}_B^{-1} - 1)\Pi, \qquad (17)$$

where $\Delta\alpha \equiv \alpha_0 - \alpha_1$, $\Delta\beta \equiv \beta_0 - \beta_1$, and

$$\alpha_{\text{eff}} = \alpha_{\text{avg}} - \frac{\Omega\theta^2}{\lambda}(\Delta\alpha)^2 - \frac{\Omega\theta^2}{\lambda}\Delta\alpha\Delta\beta,$$
$$\beta_{\text{eff}} = \beta_{\text{avg}} - \frac{\Omega\theta^2}{\lambda}(\Delta\beta)^2 - \frac{\Omega\theta^2}{\lambda}\Delta\alpha\Delta\beta. \qquad (18)$$

The quantity α_{avg} is given by $\alpha_{\text{avg}} = (k_0\alpha_0 + k_1\alpha_1)/(k_0 + k_1)$ and similar for β_{avg}. We have suppressed the explicit dependence of Π on n_A, n_B, and t to keep the notation compact.

We can interpret the reduced master equation as a set of reactions. The first two terms on the right-hand side of Eq. (17) describe particle removal, present already in the original model and independent of the state of the environment. The terms in the second line are birth reactions, as appeared originally in the model. They describe the production of single particles of type A or B. These reactions now occur with effective birth rates, indicated in Eq. (18). For a given set of model parameters these effective rates α_{eff} and β_{eff} are non-negative, provided the switching is fast enough. Given that the reduced dynamics is derived in the limit $\lambda \gg 1$, we always assume that the timescale separation λ is large enough so that $\alpha_{\text{eff}}, \beta_{\text{eff}} \geqslant 0$.

The remaining terms in Eq. (17) represent reactions which are not present in the original model; they arise from the effects of integrating out the environment. These terms represent bursting reactions; they describe events in which two particles of type A are produced simultaneously, or two particles of type B, or one of either type. This is illustrated in Fig. 1. Figure 1(a) is a schematic showing the four states that the population can reach from a given state in the next event in the original model. Figure 1(b) shows that the reduced dynamics allows three additional destinations (indicated by gray dashed arrows). The rates of the first two bursting reactions in Eq. (17) are proportional to $(\Delta\alpha)^2$ and $(\Delta\beta)^2$ and are always positive [lines three and four on the right-hand side of Eq. (17)]. The rate of the third bursting reaction [last term on the right-hand side of Eq. (17)] is positive only if $\Delta\alpha$ and $\Delta\beta$ have the same
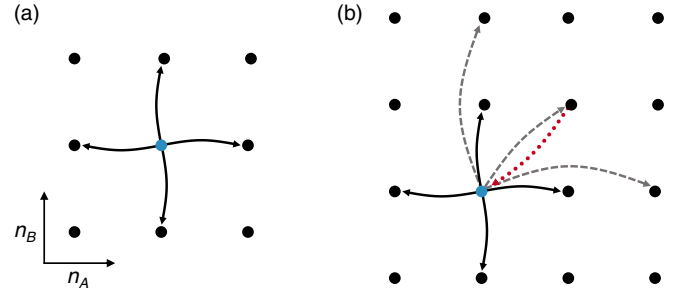

FIG. 1. Illustration of the possible reactions for (a) the model described by Eq. (16) and (b) the approximation to the model described by Eq. (17). In the original model the next event can take the population from (n_A, n_B) to four possible destinations $(n_A \pm 1, n_B)$ and $(n_A, n_B \pm 1)$. The bursting reactions in the reduced model lead to further states which can be reached, indicated by gray dashed arrows; these are $(n_A + 2, n_B)$, $(n_A, n_B + 2)$, and $(n_A + 1, n_B + 1)$. For certain choices of parameters the transition to $(n_A + 1, n_B + 1)$ can have a negative rate. In this case the flow of probability is from $(n_A + 1, n_B + 1)$ to (n_A, n_B) as indicated by the red dotted arrow; see Sec. IV A for details.

sign. We therefore distinguish between the cases $\Delta\alpha\Delta\beta > 0$ and $\Delta\alpha\Delta\beta < 0$.

2. Positive correlation between the species

In the case $\Delta\alpha\Delta\beta > 0$, the correlations between n_A and n_B are positive. There is one state of the environment which favors both species, i.e., they each have a higher birth rate in this environmental state than in the other. All rates in Eq. (17) are positive (provided λ is sufficiently large so that $\alpha_{\text{eff}}, \beta_{\text{eff}} \geqslant 0$). There is then a clear and unique way of interpreting this master equation as a continuous-time Markov process. The events described by the various terms are as above: single deaths, single births, and bursting reactions in which two particles are produced. The notion of sample paths is well defined; they can be generated using the standard Gillespie algorithm [36,37].

Some support for the validity of the reduced master equation in describing stationary states is given in Figs. 2(a)–2(c). In Fig. 2(a) we show the stationary distribution obtained from numerically integrating the full master equation (1), i.e., from the full dynamics of population and environment. This is for the case $\Delta\alpha\Delta\beta > 0$. Figure 2(b) shows the corresponding distribution from numerical integration of the reduced master equation (17). In Fig. 2(c) we have taken the adiabatic limit $\lambda \to \infty$. In each case the numerical integration is carried out using a Runge-Kutta scheme. The reduced dynamics capture the correlations between n_A and n_B in the original model; this correlation is no longer seen in the adiabatic approximation. Figure 2(d) shows the marginal distribution for the quantity $n_A + n_B$ to allow better comparison.

These observations lead to the following physical picture. In the case of infinitely fast environments (adiabatic limit) the noise from the environmental process is entirely neglected, resulting in a narrower stationary distribution [Fig. 2(d)]. In addition, our analysis shows that the environmental process introduces a positive correlation between n_A and n_B. This
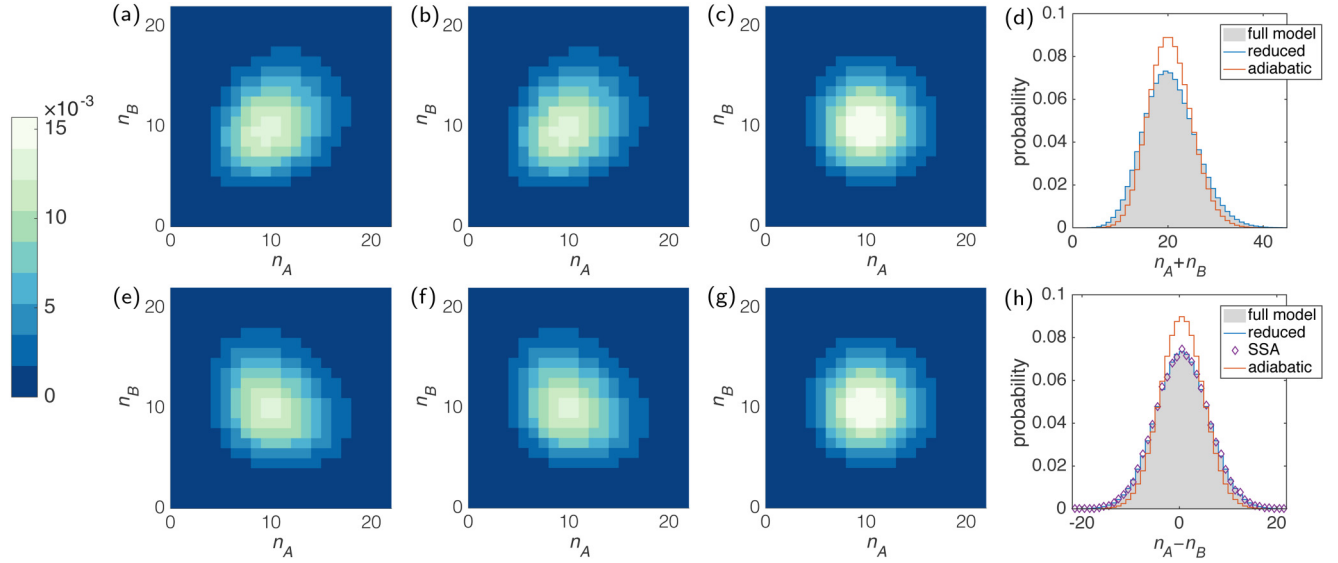
FIG. 2. Stationary distribution of the model defined in Sec. III B [see Eq. (16)] for (a)–(d) $\Delta\alpha\Delta\beta > 0$ and (e)–(h) $\Delta\alpha\Delta\beta < 0$. The distributions are obtained by numerical integration of (a) and (e) the full master equation with explicit environment, (b) and (f) the reduced master (17), and (c) and (g) the adiabatic approximation. Also shown are the marginal distribution of (d) $n_A + n_B$ and (h) $n_A - n_B$. Markers labeled SSA in (h) are from the stochastic simulation algorithm described in Appendix B 1. The parameters are (a)–(d) $\alpha_0 = 0$, $\alpha_1 = 1$, $\beta_0 = 0$, and $\beta_1 = 1$ and (e)–(h) $\alpha_0 = 0$, $\alpha_1 = 1$, $\beta_0 = 1$, and $\beta_1 = 0$. The remaining parameters are $\Omega = 20$, $\lambda = 20$, and $k_0 = k_1 = 1$.

correlation is lost in the limit of infinitely fast environmental switching.

3. Anticorrelations and negative transition rates

When $\Delta\alpha$ and $\Delta\beta$ have opposite signs, the interpretation of Eq. (17) presents an interesting feature. In this situation the (pseudo)rate of the last reaction $(\Omega^2\theta^2/\lambda)\Delta\alpha\Delta\beta$ is negative, irrespective of the value of λ. The interpretation of this term is then not clear *a priori* and Eq. (17) is not a master equation in the usual sense. We will nevertheless refer to it as the reduced master equation; a prefix "pseudo" or quotation marks are implied. Similarly, we will continue to speak of rates, even if these are negative. From Eq. (17) it is clear that negative rates of this type are present in this example if and only if $\Delta\alpha\Delta\beta < 0$.

We discuss the interpretation and limitations of the master equation with negative rates in the next section.

IV. INTERPRETATION OF NEGATIVE RATES: CONTINUOUS TIME

A. Flow of probability and renormalized reaction rates

In order to better understand a master equation with negative rates, we focus on a pair of states, which we label ℓ and ℓ', and on a single reaction of type $\ell \to \ell'$ occurring with a rate $R_{\ell\to\ell'}$. In the specific example above one would have $\ell = (n_A, n_B)$ and $\ell' = (n_A + 1, n_B + 1)$. The corresponding terms in the master equation are then

$$\frac{d}{dt}\Pi(\ell, t) = -R_{\ell\to\ell'}\Pi(\ell, t), \tag{19a}$$

$$\frac{d}{dt}\Pi(\ell', t) = R_{\ell\to\ell'}\Pi(\ell, t). \tag{19b}$$

In conventional cases the rate is positive, $R_{\ell\to\ell'} > 0$. The master equation then describes a non-negative probability flow $R_{\ell\to\ell'}\Pi(\ell)$ from ℓ to ℓ' [we suppress the time dependence of $\Pi(\ell)$ for convenience].

For $R_{\ell\to\ell'} < 0$, the flow of probability per unit time in Eqs. (19) is $|R_{\ell\to\ell'}|\Pi(\ell) \geqslant 0$ from ℓ' to ℓ. This is different from the situation in conventional Markovian systems. The flow is directed from ℓ' to ℓ, but proportional to the probability already present at ℓ. This is illustrated for the two-species model by the red arrow from $(n_A + 1, n_B + 1)$ to (n_A, b_N) in Fig. 1. Furthermore, the magnitude of this flow does not depend on $\Pi(\ell')$. Instead it is proportional to $\Pi(\ell)$, the probability of the state toward which the flow is directed. In making this argument, we have assumed $\Pi(\ell) \geqslant 0$. This assumption is not always justified in master equations with negative rates (discussed below). However, the above argument holds more generally: A negative value of $R_{\ell\to\ell'}\Pi(\ell)$ indicates a positive probability flux $|R_{\ell\to\ell'}\Pi(\ell)|$ from ℓ' to ℓ.

An approach to renormalizing master equations with negative rates has been proposed in Refs. [38,39] in the context of open quantum systems. We illustrate this using Eqs. (19), assuming again $R_{\ell\to\ell'} < 0$. For $\Pi(\ell') > 0$ we define the renormalized transition rate

$$T_{\ell'\to\ell}(t) \equiv \frac{\Pi(\ell, t)}{\Pi(\ell', t)}|R_{\ell\to\ell'}|. \tag{20}$$

The master equation (19) can be then written as

$$\frac{d}{dt}\Pi(\ell, t) = T_{\ell'\to\ell}(t)\Pi(\ell', t), \tag{21a}$$

$$\frac{d}{dt}\Pi(\ell', t) = -T_{\ell'\to\ell}(t)\Pi(\ell', t). \tag{21b}$$

Equations (21) then resemble a more traditional master equation and $T_{\ell'\to\ell}$ is the rate for transitions from ℓ' to ℓ. However, this rate depends on the probability distribution Π; in
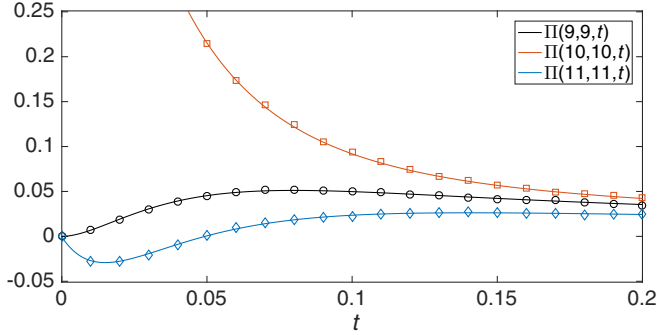
FIG. 3. Time evolution of several entries $\Pi(n_A, n_B, t)$ for the example defined in Sec. III B. The solid lines show results from integrating the reduced master equation (17), starting from a δ distribution $\Pi(n_A, n_B, t = 0) = \delta_{n_A,10}\delta_{n_B,10}$. Markers are from the numerical simulation scheme described in Appendix B 2. The model parameters are $\alpha_0 = 0, \alpha_1 = 1, \beta_0 = 1, \beta_1 = 0, \Omega = 20, \lambda = 20$, and $k_0 = k_1 = 1$.

particular $T_{\ell' \to \ell}$ is a function of $\Pi(\ell)$. This indicates non-Markovian properties [20,38,39]. The renormalized reaction rates can be used to adapt Gillespie's simulation algorithm for the generation of sample paths of stochastic systems [36,37]. We describe these adaptations in Appendix B 1. We have tested the resulting algorithm on the two-species example with $\Delta\alpha\Delta\beta < 0$ and, as seen in Fig. 2(h), it captures the anticorrelation of n_A and n_B in the stationary distribution. However, the algorithm does not reproduce all dynamical features of the original dynamics of the system and environment (see Appendix B 1). A separate sampling algorithm is described in Appendix B 2. This method simulates the solution of reduced master equations (including those with negative rates), but it does not attempt to generate sample paths.

B. Lack of positivity in initial transients

The reduced master equation (8) preserves overall probability, in the sense that $\sum_\ell \frac{d\Pi(\ell,t)}{dt} = 0$. However, if a negative rate is present, one can always find initial conditions so that negative solutions result at short times. Assume, for example, that $R_{\ell \to \ell'} < 0$ for a particular pair of states ℓ and ℓ'. We now choose the initial condition $\Pi(\ell, t = 0) = 1$ and vanishing initial probability for all other states. From Eq. (19) we then see that $\frac{d\Pi(\ell,0)}{dt} = -R_{\ell \to \ell'} > 0$ and $\frac{d\Pi(\ell',0)}{dt} = R_{\ell \to \ell'} < 0$. Thus, $\Pi(\ell', t)$ will go negative.

We have verified this by numerically integrating the reduced master equation (17). For example, if the initial condition is chosen as a δ peak concentrated on one state $\ell = (n_A, n_B)$, the numerical solution for $\Pi(n_A + 1, n_B + 1)$ is negative for a limited time as shown in Fig. 3. We analyze this further in Fig. 4, where we show the duration t^* of the initial transient in which negative probabilities are accumulated. The data suggest that this time window is limited to a duration of order λ^{-1}.

It is not surprising that Eq. (17) should become unphysical on short timescales. The typical time between switches of the environmental state is of order λ^{-1} and the reduced dynamics was derived by integrating out the fast environmental dynamics. We cannot expect Eq. (17) to resolve the physics
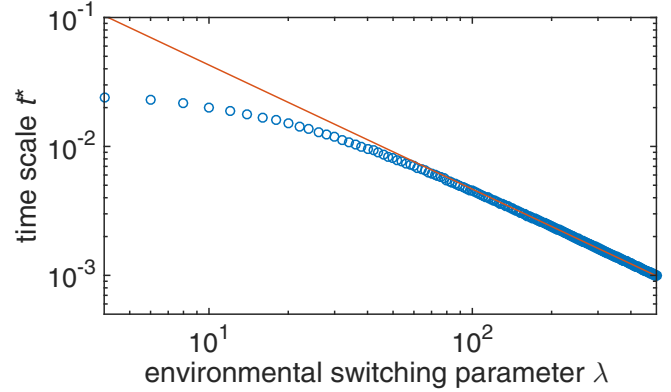

FIG. 4. Timescale t^* over which negative probabilities are accumulated. Specifically, t^* is the time at which the sum of all negative entries in Π has maximal magnitude; data are from numerical integration of Eq. (17). The solid line is a guide and corresponds to $t^* \propto 1/\lambda$. The parameters and initial condition are the same as in Fig. 3.

of the problem on timescales shorter than order λ^{-1}, as then the detailed mechanics of the environment become important. We note that negative transients have been observed before in reduced dynamics for open classical and quantum systems [40–43].

We have verified that the appearance of transient negative solutions can be cured by first integrating the full master equation describing the population and the environment for a short period of time and then subsequently changing to the reduced master equation (17). Alternatively, the reduced dynamics can be started from "slipped" initial conditions [40,42].

Parallels can be drawn between the occurrence of negative transients in reduced master equations and the well-known Pawula theorem for Kramers-Moyal expansions [44,45]. This theorem shows that carrying out a Kramers-Moyal expansion on a discrete stochastic system only produces physical results for the dynamics if the expansion truncated after terms of order one (resulting in a Liouville equation describing the deterministic flow in the limit of infinite populations) or of order two (resulting in a Fokker-Planck equation describing the diffusion approximation of the individual-based model). Truncation at any higher order can lead to negative transients. This does not, however, imply that such expansions are of no use. On the contrary, outside the initial transient a truncation to order $n \geqslant 3$ of the Kramers-Moyal expansion can produce better agreement with the probability distribution of the system that is being approximated than the traditional Fokker-Planck truncation ($n = 2$) (see Ref. [45] for details and examples). Even though the expansion may lead to unphysical results at short times, it may still be valuable at long times, for example, to calculate stationary distributions.

We have tested this for the model with two types of particles defined in Sec. III B. The stationary distribution obtained from numerical integration of the reduced master equation (17) for $\Delta\alpha\Delta\beta < 0$ captures the negative correlation of n_A and n_B in the original dynamics. This can be seen in Figs. 2(e) and 2(f). Working in the adiabatic limit, however, one finds significant deviations [Figs. 2(g) and 2(h)].

V. INTERPRETATION IN DISCRETE TIME

The results of the preceding section indicate that the reduced master equation containing negative transition rates does not have a physical interpretation at short timescales. Solutions can go negative at short times, and as a consequence reduced master equations with negative rates do not describe the statistics of a continuous-time stochastic processes. In this section we show that a valid physical reduced dynamics can be formulated for discrete time steps. To do this we look at the full dynamics of the system and environment in discrete time and provide an interpretation of the reduced dynamics at the level of discrete-time sample paths.

A. Effective time-averaged reaction rates

We focus again on the two-species example given in Sec. III. An interpretation of the terms in Eq. (17) can be obtained by looking at one sample path of the full model (population and environment) for a time interval $I \equiv [t_0, t_0 + \Delta t]$. We focus on the birth reactions. If the production rate $\Omega\alpha$ of particles of type A were constant in time, the number of birth events in the interval would be a Poissonian random variable with parameter $\Omega\alpha\Delta t$ and similarly for particles of type B (see also Ref. [46]). In the present model, the production rates are not constant as they depend on the time-dependent state of the environment. For a given trajectory of the environment we introduce the quantity

$$\overline{\alpha} = \frac{1}{\Delta t} \int_{t_0}^{t_0+\Delta t} dt' \alpha_{\sigma(t')} \tag{22}$$

and a similar definition for $\overline{\beta}$; the quantities $\Omega\overline{\alpha}$ and $\Omega\overline{\beta}$ are time-averaged production rates in the time interval I.

We note that $\overline{\alpha}$ and $\overline{\beta}$ are random variables when Δt is finite, as they depend on the random path of the environment, $\sigma(t')$, $t' \in I$. We suppress the dependence of $\overline{\alpha}$ and $\overline{\beta}$ on t_0 in our notation. The quantities $\overline{\alpha}$ and $\overline{\beta}$ will in general be correlated, as they derive from the same realization of the environment. The main principle of the calculation that follows is to approximate $\overline{\alpha}$ and $\overline{\beta}$ as correlated Gaussian random variables, while capturing their first and second moments. This Gaussian approximation is justified provided that there is a large number of switches of the environment during the time interval I, i.e., when $\lambda\Delta t \gg 1$. The number of production events of particles of type A in I can then be expected to be Poissonian with parameter $\Omega\overline{\alpha}\Delta t$ and similarly for B.

B. Averaging out the environmental process

Correlations of the environmental process decay on timescales proportional to λ^{-1}. This means that the environment is in its stationary distribution, except for a short period of order λ^{-1} at the beginning. For $\lambda\Delta t \gg 1$ this period constitutes a negligibly small fraction of the time interval, and the distribution of $\sigma(t')$ can hence be assumed to be the stationary one at all times t' during the interval. Writing $\langle\cdots\rangle$ for averages over the environmental process we have $\langle\overline{\alpha}\rangle = \alpha_{\mathrm{avg}}$ and $\langle\overline{\beta}\rangle = \beta_{\mathrm{avg}}$.

For the second moment of $\overline{\alpha}$ we find

$$
\begin{aligned}
\langle\overline{\alpha}^2\rangle &= (\Delta t)^{-2} \int_I \int_I dt\, dt' \langle\alpha_{\sigma(t)}\alpha_{\sigma(t')}\rangle, \\
&= (\Delta t)^{-2} \sum_{\sigma\sigma'} \alpha_\sigma \alpha_{\sigma'} \int_I \int_I dt\, dt' \rho[\sigma, \min(t,t')] \\
&\quad \times \rho(\sigma', |t-t'||\sigma),
\end{aligned} \tag{23}
$$

where $\rho[\sigma, \min(t,t')]$ is the probability distribution of σ at the earlier of the two times t and t'. It is given by the stationary distribution of the environment, $\rho[\sigma, \min(t,t')] = \rho^*_\sigma$, with ρ^*_σ as in Eq. (12). The notation $\rho(\sigma', \tau|\sigma)$ in Eq. (23) indicates the probability of finding the environment in state σ' if τ units of time earlier it was in state σ ($\tau > 0$). These can be obtained straightforwardly from the asymmetric telegraph process for the environment, $\rho(0, \tau|0) = \rho^*_0[1 + \frac{k_1}{k_0}e^{-\lambda(k_0+k_1)\tau}]$, and $\rho(0, \tau|1) = \rho^*_0[1 - e^{-\lambda(k_0+k_1)\tau}]$. Using this in Eq. (23) we find

$$
\begin{aligned}
\langle\overline{\alpha}^2\rangle &= \alpha_{\mathrm{avg}}^2 + \Bigg[\frac{2}{\lambda(k_0+k_1)\Delta t} + \frac{2}{\lambda^2(k_0+k_1)^2\Delta t^2} \\
&\quad \times (e^{-\lambda(k_0+k_1)\Delta t} - 1)\Bigg]\frac{k_0 k_1}{(k_0+k_1)^2}(\alpha_0 - \alpha_1)^2.
\end{aligned} \tag{24}
$$

For $\lambda\Delta t \gg 1$ the first term in the square brackets dominates relative to the second, so we can approximate

$$\langle\overline{\alpha}^2\rangle - \alpha_{\mathrm{avg}}^2 \approx \frac{\theta^2}{\lambda\Delta t}(\Delta\alpha)^2, \tag{25a}$$

with $\theta^2 = 2k_0 k_1/(k_0+k_1)^3$ as before [see Eq. (15)]. Following similar steps one finds

$$\langle\overline{\beta}^2\rangle - \beta_{\mathrm{avg}}^2 \approx \frac{\theta^2}{\lambda\Delta t}(\Delta\beta)^2, \tag{25b}$$

$$\langle\overline{\alpha}\overline{\beta}\rangle - \alpha_{\mathrm{avg}}\beta_{\mathrm{avg}} \approx \frac{\theta^2}{\lambda\Delta t}\Delta\alpha\Delta\beta. \tag{25c}$$

We therefore approximate the joint probability distribution of $\overline{\alpha}$ and $\overline{\beta}$ in the fast-switching limit as a bivariate normal distribution with these parameters.

C. Resulting event statistics

The probability that exactly m_A production events for species A occur during the time interval Δt, and m_B for species B, is given by

$$P(m_A, m_B) = \langle e^{-\Delta t\Omega(\overline{\alpha}+\overline{\beta})}\frac{(\Delta t\Omega\overline{\alpha})^{m_A}}{m_A!}\frac{(\Delta t\Omega\overline{\beta})^{m_B}}{m_B!}\rangle_{\overline{\alpha},\overline{\beta}}, \tag{26}$$

resulting from Poissonian statistics for given $\overline{\alpha}, \overline{\beta}$, subsequently averaged over the Gaussian distribution for $\overline{\alpha}$ and $\overline{\beta}$ (this average is indicated as $\langle\cdots\rangle_{\overline{\alpha},\overline{\beta}}$). Expanding in powers of

Δt, and carrying out the Gaussian average we find

$$P(m_A = 1, m_B = 0) = \Delta t \Omega \left[\alpha_{\mathrm{avg}} - \frac{\Omega \theta^2}{\lambda}(\Delta \alpha)^2 - \frac{\Omega \theta^2}{\lambda} \Delta \alpha \Delta \beta \right] - \Delta t^2 \Omega^2 (\alpha_{\mathrm{avg}}^2 + \beta_{\mathrm{avg}}^2),$$

$$P(m_A = 0, m_B = 1) = \Delta t \Omega \left[\beta_{\mathrm{avg}} - \frac{\Omega \theta^2}{\lambda}(\Delta \beta)^2 - \frac{\Omega \theta^2}{\lambda} \Delta \alpha \Delta \beta \right] - \Delta t^2 \Omega^2 (\alpha_{\mathrm{avg}}^2 + \beta_{\mathrm{avg}}^2),$$

$$P(m_A = 2, m_B = 0) = \frac{1}{2} \Delta t \frac{\Omega^2 \theta^2}{\lambda}(\Delta \alpha)^2 + \frac{1}{2} \Delta t^2 \Omega^2 \alpha_{\mathrm{avg}}^2,$$

$$P(m_A = 0, m_B = 2) = \frac{1}{2} \Delta t \frac{\Omega \theta^2}{\lambda}(\Delta \beta)^2 + \frac{1}{2} \Delta t^2 \Omega^2 \beta_{\mathrm{avg}}^2,$$

$$P(m_A = 1, m_B = 1) = \frac{\Omega^2 \theta^2}{\lambda} \Delta t \Delta \alpha \Delta \beta + \Delta t^2 \Omega^2 \alpha_{\mathrm{avg}} \beta_{\mathrm{avg}}, \tag{27}$$

where we have ignored higher-order terms (those which go like Δt^3 or $\Delta t^2/\lambda$). Larger numbers of production events ($m_A + m_B \geqslant 3$) do not contribute at this order.

It is tempting to consider the limit of infinitesimally small Δt, and to use the first-order terms in Δt in Eq. (27) to construct reaction rates. If one does so, one recovers the rates exactly as they appear in the reduced master equation (17); for example, one would infer a rate of $\frac{1}{2}(\Omega^2 \theta^2/\lambda)(\Delta \alpha)^2$ for events in which two particles of type A are produced and none of type B ($m_A = 2$ and $m_B = 0$). The rate of an event in which one A and one B are produced simultaneously would be $(\Omega^2 \theta^2/\lambda)\Delta \alpha \Delta \beta$, which is negative if $\Delta \alpha \Delta \beta < 0$.

However, taking the limit $\Delta t \to 0$ at fixed λ is not compatible with the assumption that a large number of environmental switching events occur in a given time step, i.e., $\lambda \Delta t \gg 1$. To illustrate this we carried out simulations of the full model of population and environment, and measured how many birth events of either particle type occur in a typical time interval of length Δt. Specifically we focus on the probability $P(m_A = 1, m_B = 1)$ of seeing exactly one birth event of type A and one birth event of type B during such a time interval; note that in the full model these births occur in two separate events. Results are shown in Fig. 5. The solid lines show the predictions of Eqs. (27), results from simulations of the full model are shown as markers. We first notice that simulations deviate from the results of Eqs. (27) at large values of Δt. This is to be expected as Eqs. (27) are derived neglecting

higher-order terms in Δt. Simulations and the above expressions agree to good accuracy at intermediate values of the time step; we write Δt_* for the lower end of this range, and Δt^* for the upper end. As seen in Fig. 5, the lower threshold Δt_* decreases as the switching of the environment becomes faster (i.e., λ is increased). The reduction of the threshold is in line with the requirement $\lambda \Delta t \gg 1$ for the theoretical analysis above.

When the predictions of Eqs. (27) for $P(m_A = 1, m_B = 1)$ match simulations of the full model they are largely determined by the term of order Δt^2, see again Fig. 5 (the slope of the simulation data in the log-log plot is then approximately two as indicated by the dashed lines). This term, $\Delta t^2 \Omega^2 \alpha_{\mathrm{avg}} \beta_{\mathrm{avg}}$, is positive, irrespective of the sign of $\Delta \alpha \Delta \beta$. At low values of $\Delta t \lesssim \Delta t_*$, we observe systematic deviations between simulations of the full model and the expressions in Eqs. (27). For the case $\Delta \alpha \Delta \beta < 0$ it is obvious that this must occur: at small Δt, Eqs. (27) predict $P(m_A = 1, m_B = 1) \approx (\Omega^2 \theta^2/\lambda)\Delta t \Delta \alpha \Delta \beta < 0$, whereas $P(m_A = 1, m_B = 1)$ is nonnegative in simulations by definition. Deviations at small time steps are also seen when $\Delta \alpha \Delta \beta > 0$ [see Fig. 5(a)]. The expression in Eqs. (27) shows a crossover to linear scaling in Δt, whereas simulation results scale approximately as Δt^2.

The construction in this section confirms the limitations of the reduced master equation when negative rates are present. Some of the expressions in Eq. (27) become unphysical at short timescales, just like the transient solutions of the reduced master equation. This is due to the expansion used when going from Eq. (24) to Eq. (25), where we explicitly assumed $\lambda \Delta t \gg 1$. At the same time, the discrete-time approach reveals that a physically meaningful reduced process can be defined provided Δt is not too small. We use this to describe a concrete algorithm for the simulation of discrete-time sample paths in the next section.

FIG. 5. Probability of seeing $m_A = 1$ and $m_B = 1$ in a given time interval of duration Δt. Circles show the results of simulation of the full model (population and environment); solid lines show Eq. (27). The dashed line shows a slope of 2 for comparison. Data are shown for different values of λ; all other model parameters are as in the earlier figures. Here (a) $\Delta \alpha \Delta \beta > 0$ and (b) $\Delta \alpha \Delta \beta < 0$.

D. Simulation procedure for discrete-time sample paths

The analysis of the preceding section is based on a discretization of time into intervals of length Δt. In the limit of fast switching of the environment it then assumes that the time-averaged birth rates $\Omega \overline{\alpha}$ and $\Omega \overline{\beta}$ are Gaussian random variables with statistics given in Eqs. (25). We will now use this interpretation to define an algorithm with which to
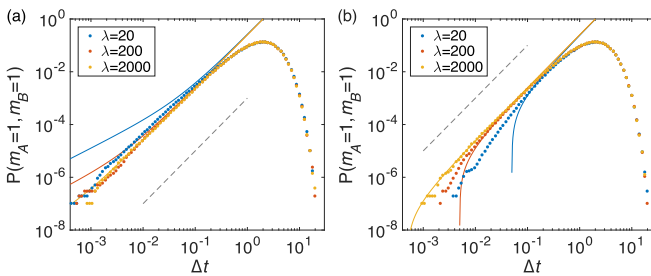
approximate sample paths of the full model in discrete time. We note that $\overline{\alpha}$ and $\overline{\beta}$ can take negative values in this Gaussian approximation. This issue arises irrespective of the sign of $\Delta\alpha\Delta\beta$ and is separate from the problem of negative rates in the reduced master equation. The probability for $\overline{\alpha}$ and/or $\overline{\beta}$ to be negative is exponentially suppressed in $\lambda\Delta t$, as the mean of the Gaussian distribution, $(\alpha_{\mathrm{avg}}, \beta_{\mathrm{avg}})$, does not depend on λ or Δt, and the covariance matrix is of order $(\lambda\Delta t)^{-1}$ [Eq. (25)]. As the switching of the environment becomes faster the distributions of $\overline{\alpha}$ and $\overline{\beta}$ become increasingly peaked around their mean. For the purposes of the numerical scheme we truncate the distribution at zero.

The algorithm uses ideas from the τ-leaping variant of the Gillespie algorithm [46], and proceeds as follows:

(1) Assume the simulation has reached time t and that the current particle numbers are n_A and n_B. Draw correlated Gaussian random numbers $\overline{\alpha}$ and $\overline{\beta}$, from a distribution with $\langle\overline{\alpha}\rangle = \alpha_{\mathrm{avg}}$, and $\langle\overline{\beta}\rangle = \beta_{\mathrm{avg}}$, and with second moments as in Eqs. (25). If $\overline{\alpha} < 0$ set $\overline{\alpha} = 0$ and similarly for $\overline{\beta}$.

(2) Using the $\overline{\alpha}$ and $\overline{\beta}$ just generated, draw independent integer random numbers m_A and m_B from Poissonian distributions with parameters $\Omega\overline{\alpha}\Delta t$ and $\Omega\overline{\beta}\Delta t$, respectively.

(3) For the death processes draw Poissonian random variables m'_A and m'_B from Poissonian distributions with parameters $\gamma n_A\Delta t$ and $\delta n_B\Delta t$, respectively.

(4) Update the particle numbers to $n_A + m_A - m'_A$ and $n_B + m_B - m'_B$, respectively (if this results in $n_A < 0$ set $n_A = 0$ and similarly for n_B).

(5) Increment time by Δt and go to 1.

We have introduced a cutoff procedure in step 4, in order to prevent particle numbers from going negative. This is necessary due to the discrete-time nature of the process, and well-known in the context of τ leaping [46]. In particular, this is not related to the appearance of negative rates in the reduced master equation, and applies in the case $\Delta\alpha\Delta\beta > 0$ as well.

We have carried out simulations using this algorithm for both cases $\Delta\alpha\Delta\beta > 0$ and $\Delta\alpha\Delta\beta < 0$. To test whether the algorithm captures dynamical properties of sample paths we have measured the power spectral density $S_{AA}(\omega) = \langle|\hat{n}_A(\omega)|^2\rangle$, where $\hat{n}_A(\omega)$ is the Fourier transform of the random process $n_A(t)$. Similarly, we also look at the cross power spectral density $S_{AB}(\omega) = \langle\hat{n}_A^\dagger(\omega)\hat{n}_B(\omega)\rangle$ (the dagger superscript denotes complex conjugation). These are the Fourier transforms of the autocorrelation and cross-correlation functions respectively.

As shown in Fig. 6 the resulting spectra of fluctuations are in agreement with those of the full model, at least to a reasonable approximation. We attribute remaining discrepancies to the discretization of time and the assumption of Gaussian effective birth rates.

It is important to stress that agreement with the full model requires a careful choice of the time step Δt. On the one hand, one needs $\Delta t \gtrsim 1/\lambda$, otherwise it is not justified to replace $\overline{\alpha}$ and $\overline{\beta}$ by Gaussian random variables. On the other hand, the so-called leap condition for τ leaping must be fulfilled [46], that is, the time step Δt must not be long enough for the population to change significantly in one step. More precisely the changes in particle numbers must remain of order Ω^0 in each step.
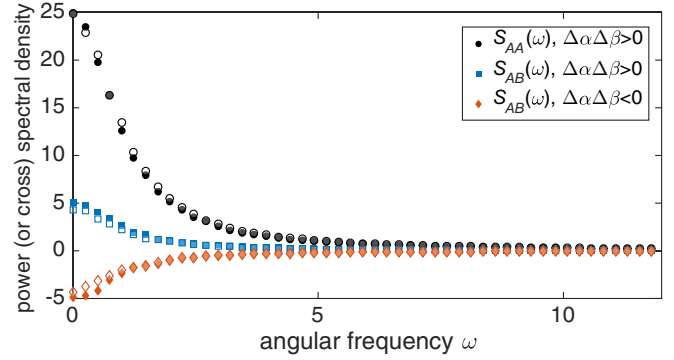

FIG. 6. Spectra of fluctuations from direct simulations of the full model (closed symbols) and using the discrete-time algorithm in Sec. V D (open symbols). The model is the same as in previous figures ($k_0 = k_1 = 1$, $\Omega = 20$, $\lambda = 20$, $\alpha_0 = 0$, $\alpha_1 = 1$, and $\Delta t = 0.1$).

VI. CRITERION FOR THE EMERGENCE OF NEGATIVE RATES

In the context of the example of Sec. III we have already established that reduced master equations with positive rates describe well-defined Markov processes. If negative rates emerge initial conditions can always be found so that negative solutions result at short times. It is therefore of primary interest to establish what properties of the original system lead to negative rates at the level of the reduced master equation.

In this section we establish a criterion for the occurrence of negative rates in equations of the type (14). It covers the class of processes in which the environmental dynamics has two states, and is independent of the state of the population. We also assume that switches of the environmental state do not change the state of the population.

A. Model and notation

We look at a general population in which each individual is of one of S species, labeled $i = 1, \dots, S$. We write n_i for the number of individuals of species i in the population, and $\mathbf{n} = (n_1, \dots, n_S)$. We label the different reactions that can occur in this system by $r = 1, 2, \dots, r_{\max}$. We write $R_{r\sigma}(\mathbf{n})$ for the rate with which reaction r occurs if the population is in state $\mathbf{n}$ and the environment in state σ.

We also introduce stoichiometric coefficients $\nu_{r,i}$, i.e., if a reaction of type r occurs, the number of particles of species i changes by $\nu_{r,i}$. These coefficients can be positive, negative or zero. We write $\boldsymbol{\nu}_r = (\nu_{r,1}, \dots, \nu_{r,S})$. In other words, if a reaction of type r occurs the state of the population changes from $\mathbf{n}$ to $\mathbf{n} + \boldsymbol{\nu}_r$. The operators $\mathcal{M}_\sigma$ are then given by

$$\mathcal{M}_\sigma = \sum_r (\mathcal{E}^{\boldsymbol{\nu}_r} - 1) R_{r\sigma}(\mathbf{n}), \tag{28}$$

where we have used the notation

$$\mathcal{E}^{\boldsymbol{\nu}} f(\mathbf{n}) = f(\mathbf{n} + \boldsymbol{\nu}), \tag{29}$$

that is to say, $\mathcal{E}^{\boldsymbol{\nu}} = \prod_i \mathcal{E}_i^{\nu_i}$, where $\mathcal{E}_i$ is the creation operator for individuals of species i.

B. Reduced master equation

The operator on the right-hand side of the reduced master equation (14) is of the form

$$\mathcal{M}_{\mathrm{red}} = \mathcal{M}_{\mathrm{avg}} + \frac{1}{2}\frac{\theta^2}{\lambda}(\mathcal{M}_0 - \mathcal{M}_1)^2, \qquad (30)$$

where $\mathcal{M}_{\mathrm{avg}} = \sum_r(\mathcal{E}^{\boldsymbol{\nu}_r} - 1)R_{r,\mathrm{avg}}(\mathbf{n})$. After some algebra we find, for the current system,

$$\mathcal{M}_{\mathrm{red}} = \sum_r(\mathcal{E}^{\boldsymbol{\nu}_r} - 1)R_{r,\mathrm{eff}}(\mathbf{n})$$

$$+ \sum_{rq}(\mathcal{E}^{\boldsymbol{\nu}_r}\mathcal{E}^{\boldsymbol{\nu}_q} - 1)R^{(rq)}(\mathbf{n}), \qquad (31)$$

where we have

$$R_{r,\mathrm{eff}}(\mathbf{n}) = R_{r,\mathrm{avg}}(\mathbf{n}) - \frac{\theta^2}{2\lambda}\Delta_r(\mathbf{n})\sum_q[\Delta_q(\mathbf{n}) + \Delta_q(\mathbf{n} - \boldsymbol{\nu}_r)],$$

$$R^{(rq)} = \frac{\theta^2}{\lambda}\Delta_r(\mathbf{n} - \boldsymbol{\nu}_q)\Delta_q(\mathbf{n}), \qquad (32)$$

with the shorthand $\Delta_r(\mathbf{n}) = R_{r,0}(\mathbf{n}) - R_{r,1}(\mathbf{n})$.

Reaction r occurs in the reduced dynamics with effective rate $R_{r,\mathrm{eff}}(\mathbf{n})$. For large enough λ, these rates are always positive. Further, one has burst reactions in the reduced dynamics. These are combinations of two original reactions r and q [see the second term on the right-hand side of Eq. (31)]. These reactions occur with rates $R^{(rq)}(\mathbf{n})$. The rates $R^{(rr)}(\mathbf{n})$ are manifestly non-negative.

Always assuming that λ is sufficiently large so that the $R_{r,\mathrm{eff}}(\mathbf{n})$ are all non-negative, we conclude that if all rates $R^{(rq)}(\mathbf{n})$ are non-negative, then the reduced master equation describes a well-defined Markov process. If this is not the case, there exist initial conditions so that the solution of the reduced master equation will have negative transients.

The criterion can be simplified further if the reactions rates do not depend on $\mathbf{n}$ (i.e., when different particles do not interact). The reduced master equation then guarantees positivity if and only if all $\Delta_r = R_{r,0} - R_{r,1}$ have the same sign (in the weak sense, some of the $\{\Delta_r\}$ may be zero). This is the case when there is one environmental state in which *all* reactions happen with a rate which is equal to or higher than in the other environmental state, i.e., if one environmental state speeds up all reactions compared to the other environment (or at least it does not make them slower).

VII. SUMMARY AND CONCLUSIONS

In summary, we have studied Markovian stochastic systems with discrete states, coupled to an external environment switching between discrete states. Our analysis focuses on the limit in which the environmental dynamics is fast relative to that of the system, but where the timescale separation is not necessarily infinite. In particular, we have derived reduced dynamics for the open system, capturing next-order corrections to the adiabatic limit.

The reduced master equation shows reactions which are not present in the original dynamics. These are bursting reactions, typically combinations of two individual reactions of the original dynamics. In some cases negative transition rates emerge.

We have demonstrated that negative (pseudo)probabilities can arise in the presence of negative rates. Numerical integration of the reduced master equation further suggests that these negative transients only occur on timescales shorter than that of the environmental process. The reduced dynamics is obtained by coarse graining the environmental process and as a consequence it does not resolve the physics of the problem on such fine timescales. Despite the unphysical transients, the reduced master equation can be useful to characterize the stationary distribution of the open system. It approximates this stationary distribution better than an adiabatic approach, in which the timescale separation is assumed to be infinite.

The emergence of bursting reactions can be understood further by looking at the time evolution of individual sample paths of system and environment over a finite time interval. This leads to a discrete-time approximation for the dynamics of the open system. The path of the environment in one time step can be approximated by Gaussian random variables; bursting in the system results from fluctuations of this discrete-time Gaussian process. We have used this approach to propose a simulation method for stochastic systems coupled to a fast-switching environment with two states.

We note that Refs. [8,10,16,23,24] use the Wentzel-Kramers-Brillouin (WKB) method to calculate stationary distributions of populations with fast environmental dynamics. While some dynamical properties can be derived from this (e.g., mean first-passage times), the method is not in itself a dynamic approach. It does not provide immediate access to two-time objects such as correlation functions. Our approach is different; it reduces the dynamics of the system by integrating out the environment. The result is a dynamical process. For example, we study spectra of fluctuations in Fig. 6 (see also Fig. 7 in Appendix B). We also note that the WKB approach is based on a limit of large population size and that it often requires the existence of fixed points of the limiting deterministic model. In our derivation of the reduced master equation we have not made these assumptions.

Negative rates can also be found in the reduced dynamics for open quantum systems. In this context one starts from a unitary dynamics of the system and environment [20,21]. Upon tracing out the environment a quantum master equation with temporarily negative decay rates can result. We note one potentially important difference between the classical and the quantum cases; the origin of negative rates in open quantum systems is often attributed to a two-way exchange of information between the system and the environment [20,21]. This mechanism is not available for the two-species example we have looked at (Sec. III). Still, the reduced master equation for this model can have negative rates.

Our work provides several starting points for future work. In the following paper [31] we build on the reduction technique developed herein by combining it with approximations to the dynamics of the population itself through expansions in the inverse system size. We describe a number of weak-noise expansions which allow for analytical results or more efficient simulation. The construction in Sec. V and the associated discrete-time simulation algorithm could be extended to more general models with multiple environmental states. This could provide a powerful tool for the simulation of systems coupled to fast external environments. Further, it would be interesting

to study in more detail the analogies and differences between the reduced dynamics for open quantum systems and for classical systems coupled to fast environments. As a first step, one might focus on classical systems in which the dynamics of the environment depends on the state of the system itself and try to characterize the information flow between the system and environment. A separate further line of research might focus on systems in which the environment takes continuous states (see, e.g., Ref. [10,23,24]) and on the comparison with the discrete case.

ACKNOWLEDGMENTS

APPENDIX A: STATE-DEPENDENT ENVIRONMENTAL PROCESS

We briefly consider the case in which the transition matrix for the environmental process depends on the state of the system proper, i.e., $A_{\sigma \to \sigma'} = A_{\sigma \to \sigma'}(\ell)$. From Eq. (8) we have

$$\frac{d}{dt}\Pi(\ell, t) = \sum_\sigma \mathcal{M}_\sigma[\rho^*(\sigma|\ell)\Pi(\ell, t)] + \frac{1}{\lambda}\sum_\sigma \mathcal{M}_\sigma w_\sigma(\ell, t)$$

(A1)

and from Eq. (9)

$$\sum_{\sigma'} A_{\sigma' \to \sigma}(\ell)w_{\sigma'}(\ell, t)$$
$$= \rho^*(\sigma|\ell)\sum_{\sigma'} \mathcal{M}_{\sigma'}[\rho^*(\sigma'|\ell)\Pi(\ell, t)]$$
$$- \mathcal{M}_\sigma[\rho^*(\sigma|\ell)\Pi(\ell, t)].$$

(A2)

1. Adiabatic limit

It is useful to define the operators, acting on functions $f(\ell)$,

$$\widehat{\mathcal{M}}_\sigma f(\ell) = \mathcal{M}_\sigma[\rho^*(\sigma|\ell)f(\ell)],$$

(A3)

where the right-hand side indicates that the operator $\mathcal{M}_\sigma$ acts on the object inside the square brackets. In the adiabatic limit one finds [by sending $\lambda \to \infty$ in Eq. (A1)]

$$\frac{d}{dt}\Pi(\ell, t) = \widehat{\mathcal{M}}_{\text{avg}}\Pi(\ell, t),$$

(A4)

where we now have

$$\mathcal{M}_{\text{avg}} = \sum_\sigma \widehat{\mathcal{M}}_\sigma.$$

(A5)

To illustrate the principle we use a population with n individuals of a single species and a birth reaction with rate $b_\sigma(n)$, which may potentially depend on n. We then have $\mathcal{M}_\sigma = [\mathcal{E}^{-1} - 1]b_\sigma(n)$. We find

$$\mathcal{M}_{\text{avg}}\Pi(n, t) = [\mathcal{E}^{-1} - 1]b_{\text{avg}}(n)\Pi(n, t),$$

(A6)

where

$$b_{\text{avg}}(n) = \sum_\sigma \rho^*(\sigma|n)b_\sigma(n).$$

(A7)

We note that $b_{\text{avg}}(n)$ carries a dependence on n, even when $b_\sigma(n)$ is itself independent of n.

2. Next-order contribution

We focus on the case of two environmental states, with switching rates $A_{1 \to 0}(\ell) = k_0(\ell)$ and $A_{0 \to 1}(\ell) = k_1(\ell)$. In this case we have $\rho^*(0|\ell) = k_0(\ell)/[k_0(\ell) + k_1(\ell)]$ and $\rho^*(1|\ell) = k_1(\ell)/[k_0(\ell) + k_1(\ell)]$. From Eq. (A2) we then find

$$w_0(\ell, t) = -w_1(\ell, t) = \frac{1}{k_0(\ell) + k_1(\ell)}[\rho^*(1|\ell)\widehat{\mathcal{M}}_0 - \rho^*(0|\ell)\widehat{\mathcal{M}}_1]\Pi(\ell, t).$$

(A8)

Inserting into Eq. (A1) we have

$$\frac{d}{dt}\Pi(\ell, t) = \mathcal{M}_{\text{avg}}\Pi(\ell) + \frac{1}{\lambda}(\mathcal{M}_0 - \mathcal{M}_1)\frac{1}{k_0(\ell) + k_1(\ell)}[\rho^*(1|\ell)\widehat{\mathcal{M}}_0 - \rho^*(0|\ell)\widehat{\mathcal{M}}_1]\Pi(\ell, t),$$

(A9)

which can be written as

$$\frac{d}{dt}\Pi(\ell, t) = \mathcal{M}_{\text{avg}}\Pi(\ell) + \frac{1}{\lambda}[\widehat{\mathcal{M}}_0\rho^*(0|\ell)^{-1} - \widehat{\mathcal{M}}_1\rho^*(1|\ell)^{-1}]\frac{1}{k_0(\ell) + k_1(\ell)}[\rho^*(1|\ell)\widehat{\mathcal{M}}_0 - \rho^*(0|\ell)\widehat{\mathcal{M}}_1]\Pi(\ell, t).$$

(A10)

While this object is quite lengthy, it formally describes the reduced dynamics to subleading order in $1/\lambda$ and can be used for further analysis.

APPENDIX B: CONTINUOUS-TIME SIMULATION ALGORITHMS FOR REDUCED MASTER EQUATIONS WITH NEGATIVE RATES

1. Path-level simulation

a. Description of the simulation algorithm

A stochastic simulation algorithm was discussed in Ref. [38] for non-Markovian jumps in quantum systems.

This method simulates processes defined by quantum master equations with temporarily negative decay rates. The central idea is to represent the solution of the master equation by an ensemble of sample paths, which are generated *in parallel*. In contrast with standard methods [36,37], these paths are correlated with each other.

We have adapted the algorithm to the case of the classical master equation

$$\frac{d}{dt}\Pi(\ell, t) = \sum_{\ell'} R_{\ell' \to \ell}\Pi(\ell', t),$$
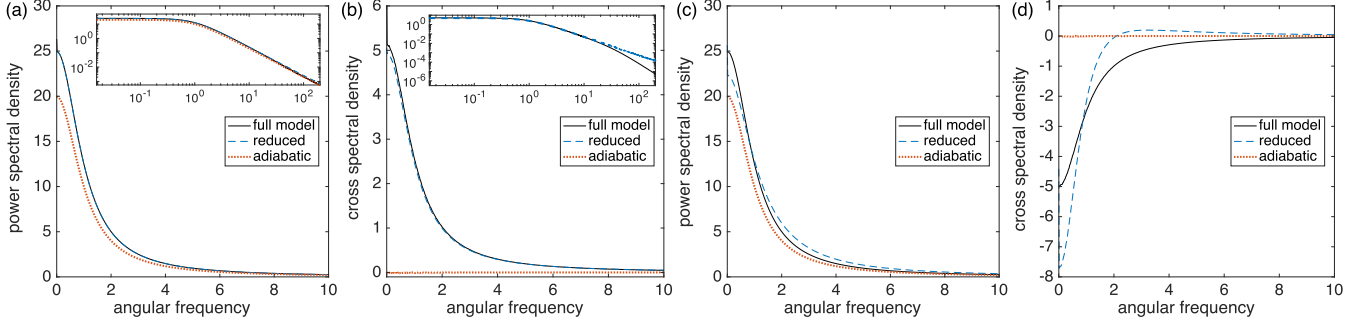
(B1)

FIG. 7. Spectra of fluctuations for the model defined in Sec. III B for (a) and (b) $\Delta\alpha\Delta\beta > 0$ and (c) and (d) $\Delta\alpha\Delta\beta < 0$. We show (a) and (c) the power spectral density $S_{AA}(\omega)$ and (b) and (d) the cross spectral density $S_{AB}(\omega)$; the insets show the same quantities on a logarithmic scale. The parameters are $\alpha_0 = 0$, $\alpha_1 = 1$, $\lambda k_0 = \lambda k_1 = 20$, $\Omega = 20$, and (a) and (b) $\beta_0 = 0$ and $\beta_1 = 1$ and (c) and (d) $\beta_0 = 1$ and $\beta_1 = 0$.

where some of the rates $R_{\ell'\to\ell}$ may be negative. The algorithm uses Eqs. (20) and (21) to convert reactions with negative rates into reactions in the opposite direction and with positive renormalized rates. In order to do this we need the entries of the probability distribution $\Pi(\ell)$ and $\Pi(\ell')$ [see Eq. (20)]. These in turn are estimated from the ensemble of sample paths. In this way, the trajectories are correlated with each other [38,39].

We index each trajectory individually so that we can follow the time evolution of each sample path. At each point in time the ensemble is specified by the state of each of the sample paths. We write N_ℓ for the number of sample paths in state ℓ. To keep the notation compact we suppress the time dependence of N_ℓ. One has $\sum_\ell N_\ell = M$ at all times, where M is the size of the ensemble.

Before we detail the algorithm we describe the construction of a matrix $\mathbf{S}$ with elements $S_{\ell\to\ell'}$ which give the rate of a reaction $\ell \to \ell'$ to occur *in the ensemble*. The matrix is needed frequently in the algorithm and is constructed as follows. (i) Start with $S_{\ell\to\ell'} = 0$ for all ℓ and ℓ'. (ii) For all reactions $\ell \to \ell'$ with positive rate $R_{\ell\to\ell'}$ increase $S_{\ell\to\ell'}$ by $R_{\ell\to\ell'}$. (iii) For reactions with negative rate $R_{\ell\to\ell'}$ and $N_{\ell'} > 0$ construct $T_{\ell'\to\ell}$ as in Eq. (20), where $N_\ell/N_{\ell'}$ is used as a proxy for $\Pi(\ell)/\Pi(\ell')$. If $N_{\ell'} = 0$ set $T_{\ell'\to\ell} = 0$. Increase $S_{\ell\to\ell'}$ by $T_{\ell'\to\ell}$. (iv) Finally, for all pairs ℓ and ℓ' multiply $S_{\ell\to\ell'}$ by N_ℓ. For a given master equation (i.e., a given matrix $\mathbf{R}$) the matrix $\mathbf{S}$ is a function of the current state of the ensemble, i.e., of the $\{N_\ell\}$. All entries $S_{\ell\to\ell'}$ ($\ell \neq \ell'$) are non-negative. The diagonal elements are zero. The element $S_{\ell\to\ell'}$ indicates the rate for a reaction $\ell \to \ell'$ to occur, given the current state of the ensemble. One has $S_{\ell\to\ell'} = 0$ if no sample path in the ensemble is in state ℓ. We also note that the total rate for a reaction of any type to happen $\sum_{\ell\neq\ell'} S_{\ell\to\ell'}$ scales linearly with M. This guarantees that each time step in the procedure below is of order M^{-1} or, in other words, that order M reactions occur per unit time.

The algorithm proceeds as follows:

(1) Given the current state of the ensemble, compute the matrix $\mathbf{S}$ as described above.

(2) Draw a random time increment τ from an exponential distribution with parameter $s = \sum_{\ell,\ell'} S_{\ell\to\ell'}$.

(3) Randomly select an origin ℓ and a destination ℓ' with a probability weighted by $S_{\ell\to\ell'}$ (i.e., the probability that ℓ is picked as an origin and ℓ' as a destination is $S_{\ell\to\ell'}/s$).

(4) Randomly (with equal probabilities) pick one of the sample paths currently in state ℓ and change its state to ℓ'.

(5) Increment time by τ and go to step 1.

We note that this algorithm does not allow for any state ℓ to ever have a negative occupancy N_ℓ. Furthermore, if all $R_{\ell\to\ell'}$ are non-negative the simulation reduces to the standard Gillespie algorithm [36,37]. In this case the sample paths remain uncorrelated.

b. Test of the algorithm

Here we show that this method can fail to produce sample paths which are representative of the full model. We use the example in Eq. (17). The algorithm captures the stationary distribution accurately, as illustrated by the markers in Fig. 2(h). Next we test whether the simulation reproduces dynamical properties of the sample paths of the full model. Specifically, we focus on the power and cross spectra defined in Sec. V D.

Results are shown in Fig. 7. These are measured in the regime when $\Pi(n_A, n_B)$ has reached the stationary state and are averaged over a large ensemble of trajectories.

i. Only positive rates in the reduced master equation. Figures 7(a) and 7(b) serve as a benchmark and show the case $\Delta\alpha\Delta\beta > 0$ when all rates in the reduced master equation are positive. The above simulation scheme then reduces to the standard Gillespie method. As seen in the figure, the power and cross spectra $S_{AA}(\omega)$ and $S_{AB}(\omega)$ obtained from simulating paths of the reduced master equation agree well with those from simulations of the full model, at least at sufficiently low frequencies ω. At larger frequencies deviations are seen; this is particularly visible for the cross spectrum [see the inset of Fig. 7(b)]. These deviations between reduced and the full model are not surprising; the reduced model does not resolve the mechanics of the environment on short timescales. Spectra obtained from sample paths of the master equation in the adiabatic limit show significant deviations from those of the full model; we note in particular that the cross spectrum $S_{AB}(\omega)$ vanishes [dotted red line in Fig. 7(b)].

ii. Negative rates. Results for the case with negative rates in the reduced master equation are shown in Figs. 7(c) and 7(d). We find marked differences between the spectra generated from the reduced master equation with the above algorithm

and those of sample paths of the full model. This is particularly noticeable in the cross spectrum in Fig. 7(d), which is strictly negative in the full model, but comes out positive at intermediate frequencies if the above simulation method is used for the reduced dynamics.

We conclude that the trajectories generated by the simulation algorithm in Appendix B 1 a do not represent sample paths of the full model when the reduced master equation contains negative rates. Our findings invite the question whether algorithms of this type [38,39] provide a faithful representation of the full dynamics of open quantum systems and their environment.

2. Distribution-level simulation

The time-dependent solution $\Pi(\ell, t)$ can be obtained by direct numerical integration of the reduced master equation, for example, using a Runge-Kutta scheme. However, for large state spaces this approach can become slow. The technique described in this section can, in some cases, provide a faster alternative.

We consider a large number M of discrete units of probability $1/M$. At each point in time the state of the simulation is defined by the occupation numbers N_ℓ for all states ℓ; some of the N_ℓ may be negative. One has $\sum_\ell N_\ell = M$.

The algorithm proceeds along the following steps:

(1) For given occupation numbers N_ℓ at time t, make a list of all possible reactions, labeled by index γ. Each reaction has a site of origin ℓ_γ, a destination site ℓ'_γ, and rate $r_\gamma = R_{\ell_\gamma \to \ell'_\gamma} N_{\ell_\gamma}$. Some of the r_γ may be negative.

(2) Draw a random number τ from an exponential distribution with parameter $\sum_\gamma |r_\gamma|$.

(3) Pick a reaction from the list created in step 1. The probability to pick γ is $|r_\gamma|/\sum_{\gamma'} |r_{\gamma'}|$.

(4) If $r_\gamma > 0$ increase $N_{\ell'_\gamma}$ by one and reduce N_{ℓ_γ} by one. If $r_\gamma < 0$ reduce $N_{\ell'_\gamma}$ by one and increase N_{ℓ_γ} by one.

(5) Increment time by τ and go to step 1.

The process in step 4 allows occupation numbers to go negative. The typical time step of this scheme is given by $1/\sum_\gamma |r_\gamma|$, and reaction γ is triggered with probability $|r_\gamma|/(\sum_{\gamma'} |r_{\gamma'}|)$. Thus $|r_\gamma|$ reactions of type γ are triggered per unit time. The sign convention in step 4 ensures correct sampling of the reduced master equation.

We tested this procedure for the example given by Eq. (17). Results are shown in Fig. 3; there is near perfect agreement between the Monte Carlo procedure and direct numerical integration of the reduced master equation. We stress that this algorithm does not generate sample paths for the reduced master equation.

[1] E. Kussell, R. Kishony, N. Q. Balaban, and S. Leibler, Genetics **169**, 1807 (2005).

[2] E. Kussell and S. Leibler, Science **309**, 2075 (2005).

[3] S. Leibler and E. Kussell, Proc. Natl. Acad. Sci. USA **107**, 13183 (2010).

[4] P. Thomas, N. Popović, and R. Grima, Proc. Natl. Acad. Sci. USA **111**, 6994 (2014).

[5] T. B. Kepler and T. C. Elston, Biophys. J. **81**, 3116 (2001).

[6] M. Thattai and A. Van Oudenaarden, Genetics **167**, 523 (2004).

[7] P. S. Swain, M. B. Elowitz, and E. D. Siggia, Proc. Natl. Acad. Sci. USA **99**, 12795 (2002).

[8] M. Assaf, E. Roberts, Z. Luthey-Schulten, and N. Goldenfeld, Phys. Rev. Lett. **111**, 058102 (2013).

[9] A. Duncan, S. Liao, T. Vejchodský, R. Erban, and R. Grima, Phys. Rev. E **91**, 042111 (2015).

[10] M. Assaf, M. Mobilia, and E. Roberts, Phys. Rev. Lett. **111**, 238101 (2013).

[11] P. Ashcroft, P. M. Altrock, and T. Galla, J. R. Soc. Interface **11**, 20140663 (2014).

[12] K. Wienand, E. Frey, and M. Mobilia, Phys. Rev. Lett. **119**, 158301 (2017).

[13] R. West, M. Mobilia, and A. M. Rucklidge, Phys. Rev. E **97**, 022406 (2018).

[14] A. J. Black and A. J. McKane, J. Theor. Biol. **267**, 85 (2010).

[15] C. Escudero and J. Á. Rodríguez, Phys. Rev. E **77**, 011130 (2008).

[16] M. Assaf, A. Kamenev, and B. Meerson, Phys. Rev. E **78**, 041123 (2008).

[17] Q. Luo and X. Mao, J. Math. Anal. Appl. **334**, 69 (2007).

[18] C. Zhu and G. Yin, J. Math. Anal. Appl. **357**, 154 (2009).

[19] H.-P. Breuer and F. Petruccione, *The Theory of Open Quantum Systems* (Oxford University Press, Oxford, 2002).

[20] H.-P. Breuer, E.-M. Laine, J. Piilo, and B. Vacchini, Rev. Mod. Phys. **88**, 021002 (2016).

[21] I. de Vega and D. Alonso, Rev. Mod. Phys. **89**, 015001 (2017).

[22] P. C. Bressloff, Phys. Rev. E **94**, 042129 (2016).

[23] M. Assaf, E. Roberts, and Z. Luthey-Schulten, Phys. Rev. Lett. **106**, 248102 (2011).

[24] E. Roberts, S. Be'er, C. Bohrer, R. Sharma, and M. Assaf, Phys. Rev. E **92**, 062717 (2015).

[25] P. C. Bressloff and J. M. Newby, Phys. Rev. E **89**, 042701 (2014).

[26] P. C. Bressloff, Phy. Rev. E **95**, 012124 (2017).

[27] P. C. Bressloff, Phys. Rev. E **95**, 012138 (2017).

[28] P. C. Bressloff, Phys. Rev. E **95**, 012130 (2017).

[29] J. Bowen, A. Acrivos, and A. Oppenheim, Chem. Eng. Sci. **18**, 177 (1963).

[30] L. A. Segel and M. Slemrod, SIAM Rev. **31**, 446 (1989).

[31] P. G. Hufton, Y. T. Lin, and T. Galla, Phys. Rev. E **99**, 032122 (2019).

[32] W. Ewens, *Mathematical Population Genetics 1* (Springer, New York, 2004).

[33] A. Traulsen and C. Hauert, in *Reviews of Nonlinear Dynamics and Complexity*, edited by H. G. Schuster (Wiley-VCH, Weinheim, 2010), pp. 25–61.

[34] J. M. Sancho and M. San Miguel, J. Stat. Phys. **37**, 151 (1984).

[35] E. Hernández-García, L. Pesquera, M. A. Rodríguez, and M. San Miguel, J. Stat. Phys. **55**, 1027 (1989).

[36] D. T. Gillespie, J. Comput. Phys. **22**, 403 (1976).

[37] D. T. Gillespie, J. Chem. Phys. **81**, 2340 (1977).

[38] J. Piilo, S. Maniscalco, K. Härkönen, and K.-A. Suominen, Phys. Rev. Lett. **100**, 180402 (2008).

[39] H.-P. Breuer and J. Piilo, Europhys. Lett. **85**, 50004 (2009).

[40] A. Suárez, R. Silbey, and I. Oppenheim, J. Chem. Phys. **97**, 5101 (1992).

[41] P. Pechukas, Phys. Rev. Lett. **73**, 1060 (1994).

[42] S. Gnutzmann and F. Haake, Z. Phys. B **101**, 263 (1996).

[43] F. Benatti, R. Floreanini, and M. Piani, Phys. Rev. A **67**, 042110 (2003).

[44] R. F. Pawula, Phys. Rev. **162**, 186 (1967).

[45] H. Risken and H. Vollmer, Z. Phys. B **35**, 313 (1979).

[46] D. T. Gillespie, J. Chem. Phys. **115**, 1716 (2001).